

# SHEAR BEHAVIOR OF RC BEAMS STRENGTHENED BY CFRP GRID AND SPRAYED MORTAR

Vu Dung TRAN<sup>\*1</sup>, Kimitaka UJI<sup>\*2</sup>, Bo WANG<sup>\*3</sup>, Ngoc Linh VU<sup>\*4</sup>

## ABSTRACT

The shear failure of reinforced concrete (RC) beams is particularly dangerous due to occurring suddenly and hard to predict. In the experimental study, three RC beams were fabricated. To improve shear capacity, two of these beams were strengthened by using carbon fiber-reinforced polymer (CFRP) grid and sprayed mortar. The four-points bending test were carried out in all beams. Next, the corresponding models in 3D finite-element method (FEM) were simulated. There is a good agreement between simulations and experiments about the load capacity, the failure process and effects of the repair method. **Keywords:** shear failure, RC beam, CFRP grid, sprayed mortar, finite element modelling, Marc-Mentat

## 1. INTRODUCTION

Concrete structures plays a major role in the infrastructure of all nations. After the construction boom in many countries in the middle of last century, many concrete structures become severely damage after a long time service. There are various studies on how to repair such aged structures. In recent years, CFRP materials are widely used as reinforcement owing to their anticorrosion properties and high tensile strength. Especially, CFRP grid presents many advantages in term of erection in comparison with CFRP sheet. However, the majority of the studies have focused on the use of CFRP sheets to strengthen beams or slabs under bending load, whereas the use of CFRP grids to improve shear failure resistance is not adequately studied [1].

Japan is an earthquake-prone country with a long coastline. Therefore, reinforcements in a RC beam can be corroded easily due to water ingress through small cracks. Especially, corrosion in the stirrups, which are the reinforcing bars nearest the external surface of RC beam, can causes the brittle fracturing in shear mode. The shear failure of an RC beam, which is more dangerous than flexural failure, is still not well-understood [2]. If the beam design does not call for adequate shear reinforcements, then overloading will induce shear collapse. A superior alternative protection method is to combine CFRP materials with cement layers.

In this study, experiments and FEM models evaluate the effects of shear reinforcement and CFRP grid combined with a mortar layer in three RC beams, which differ in shear reinforcements' arrangement. The results explain more detail about the shear failure process and the influence of repair material to load capacity of these beams.

Table 1 Mix proportion of concrete

G	SL	W/C	Air	Unit weight (kg/m <sup>3</sup> )					
(mm)	(mm)	(%)	%	W	C	S	G1	G2	Ad*
20	120	55.6	4.5	158	284	792	796	330	1.3

\*Ad: Water reducing and air entraining admixture

Table 2 Properties of concrete and mortar

Type	Compressive strength (N/mm <sup>2</sup> )	Elastic modulus (kN/mm <sup>2</sup> )	Tensile strength (N/mm <sup>2</sup> )	Shear Strength of interface (N/mm <sup>2</sup> )
Concrete	34.1	31.9	2.92	4.75
Mortar	36.7	31.0	2.87	

Table 3 Properties of reinforcements and CFRP

Rebar	Type	Area (mm <sup>2</sup> )	Yield stress (N/mm <sup>2</sup> )	Tension strength (N/mm <sup>2</sup> )
	D32	794.2	389	587
D10	71.33	413	561	
D6	31.67	417	570	
CFRP	Type	Area (mm <sup>2</sup> )	Tension strength (N/mm <sup>2</sup> )	Elastic modulus (kN/mm <sup>2</sup> )
	CR8	26.5	1400	100

## 2. EXPERIMENTAL STUDY

### 2.1 Materials and mix proportions

All three RC beams were cast using the ready mix concrete with the compressive strength of 34.1 N/mm<sup>2</sup> and the maximum aggregate size of 20 mm. In the mix

\*1 PhD student, Dept. of Civil and Environmental Engineering, Tokyo Metropolitan Uni., JCI Student Member

\*2 Prof., Dept. of Civil and Environmental Engineering, Tokyo Metropolitan Uni., Dr.E., JCI Member

\*3 PhD student, Dept. of Civil and Environmental Engineering, Tokyo Metropolitan Uni., JCI Student Member

\*4 PhD student, Dept. of Civil and Environmental Engineering, Tokyo Metropolitan Uni.

Table 4 Detail of shear reinforcements in beams

No.	Shear reinforcements	Total reinforcement area (mm <sup>2</sup> /200mm)
RC1	D10-SD345 @200mm	142.66
RC2	D6-SD345 @200 + CR8 @100mm	169.34
RC3	CR8 @100mm	106

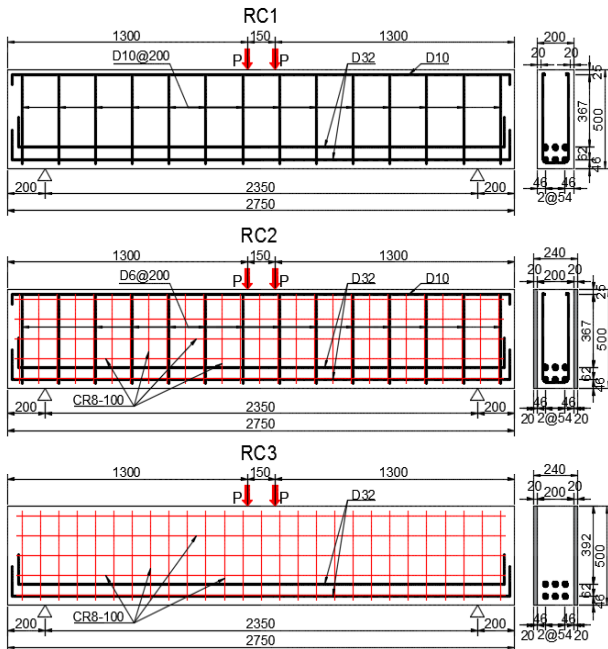


Fig.1 Dimensions and reinforcement arrangement

proportion of concrete, high early-strength Portland cement was used and water-cement ratio was 0.556 (Table 1).

Sprayed mortar is a polymer-modified cement with the proportion of premixed mortar, shot polymer and water was 25kg, 1.21kg and 4.1kg, respectively. The shear strength of the interface between mortar and concrete was determined from a direct shear test. To improve the adhesion of the interface, an Epoxy primer was applied.

D32 was the main steel rebar and D6, D10 were the stirrups and reinforcing steel in the compressive zone. CFRP-CR8 with grid spacing of 100x100 mm were used to increase shear resistance capacity of these beams. The mechanical properties of these materials are given in Table 2 and 3. The values of concrete, mortar and steel rebar are obtained from the actual corresponding tests. The values of CFRP is obtained from its product catalog.

## 2.2 Test specimens

To evaluate the shear resistance capacity of sprayed mortar and CFRP grid, the experimental program consists three types of RC beam specimens of that be different in the arrangements of strengthened materials (Fig. 1 & Table 4). The first beam, named RC1, is a normal RC beam with the sizes of 2750x500x200 mm. This beam used D32 bar as the main



a, Arrangement of reinforcements



b, Casting in the wooden mold



c, Placing CFRP Grid and spraying Epoxy Primer



d, Spraying polymer mortar

Fig. 2 Making an RC beam

reinforcements, D10 bar as the compression reinforcements and the stirrups was D10 with 200 mm spacing. The RC2 beam were strengthened by CFRP grid and sprayed mortar. CFRP frame were attached along the substrate beam's webs and then sprayed mortar to create 20mm repair layer at the each side. With the assumption that the shear reinforcement in this beam lost its area due to corrosion, the stirrups in RC2 used D6 bar, which is smaller than in the RC1's. On the other hand, the RC3 beam also had CFRP-mortar layer like in the RC2 but



Fig. 3: Four point bending test

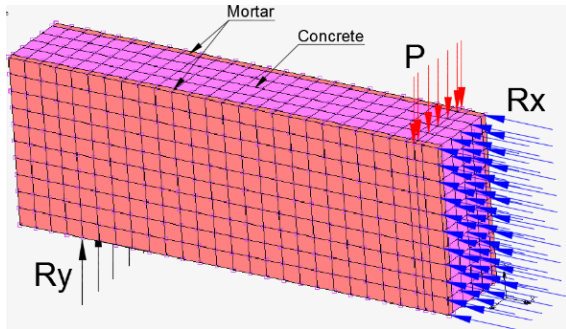


Fig. 4: FEM model of an RC beam

did not use any stirrup and compression reinforcements.

### 2.3 Casting RC beams

Firstly, three substrate concrete beams were cast in wooden molds and then curing by moisture-retaining cover. Eight days after making the substrate beams, RC2 and RC3's web surface were sand blasted. Four days later, CFRP grid were placed on these beam's web surface by using steel bolt anchors. In the next day, an epoxy primer was applied and the repair mortar was sprayed after epoxy layer had dried. Lastly, a curing compound was sprayed on the mortar surface. The tests were carried out at the age of 26, 27, 29 days of the substrate beams, respectively. Fig. 2 shows the specimens fabrication procedure.

### 2.4 Test procedure

The four-points bending test was carried out in all specimens (Fig. 3). During test, when appearing the first flexural crack and the first diagonal crack, the specimens were unloaded to mark the cracks and take photographs. After that, the load increased until the specimens failed. The loading rate of RC1 before appearing flexural cracks is 4 kN/min and after that is 6 kN/min. The loading rate of the beams RC2, RC3 is maintained at 8kN/min. In the tests, the failure processes were monitored by using strain gauges on the reinforcements, CFRP grid and acoustic emission (AE) sensors on the beam's surface. The AE data were analyzed by using simplified Green's functions and the moment tensor analysis (SiGMA) procedure [3].

## 3. FEM ANALYSIS

With the aim of evaluation the capacity of the RC

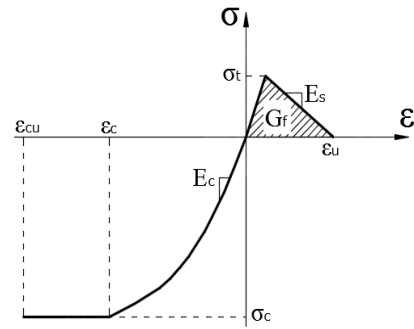


Fig. 5: Constitutive of concrete

beams, differ in shear reinforcements, a nonlinear finite element analysis by means of a MSC Marc-Mentat software was applied [4]. The three-dimensional RC beam's finite element model was created and simulated the four-point bending test. Because of symmetry, only a half of the beams were simulated in the models (Fig. 4). The mesh is divided to 50mm for each element's size. The mesh size should be a divisor of the CFRP grid spacing (100x100mm); and fine enough for analyzing to get accurate results but not take a long computing time. In RC1, 1732 nodes and 1306 elements are used; in RC2, 3104 nodes and 2080 elements are used; whereas the numbers of RC3 are 3014 nodes and 1950 elements. Indeed, many factors influence the bearing capacity of reinforced concrete members. Therefore, these factors will be estimated appropriately with analytical ideas in the following parts.

### 3.1 Constitutive modelling

#### (1) Concrete and mortar

An elastic-plastic isotropic material with smeared-cracking model can simulate the behavior of concrete and mortar components. Element type 7, which is an eight-node, iso-parametric, arbitrary hexahedral, was used to model the concrete and mortar elements.

The crack modelling was defined by the Damage/Cracking function of Marc-Mentat. The cracking data is presented in Fig. 5. The critical cracking stress is set as tension strength of the materials  $\sigma_t$ . The choice of a value of the tension softening modulus can be related to on the fracture energy  $G_f$ . According to Vos [5], the fracture energy  $G_f$  is:

$$G_f = 25 \cdot \sigma_t \quad (\text{N/m}) \quad (1)$$

Where,

$\sigma_t$ : tensile strength ( $\text{N/mm}^2$ ).

Assuming that the micro-cracks are uniformly distributed over the specimen length  $l_s$ , so that

$$G_f = 1/2 \cdot l_s \cdot \sigma \cdot \epsilon_u \quad (\text{N/m}) \quad (2)$$

Where,

$l_s$ : specimen length, equal 50 mm.

$\epsilon_u$ : ultimate tension strain

From these Eq. (1), (2), the value  $\epsilon_u$  can calculate ( $\approx 0.001$ ) and the tension softening modulus  $E_s$  is:

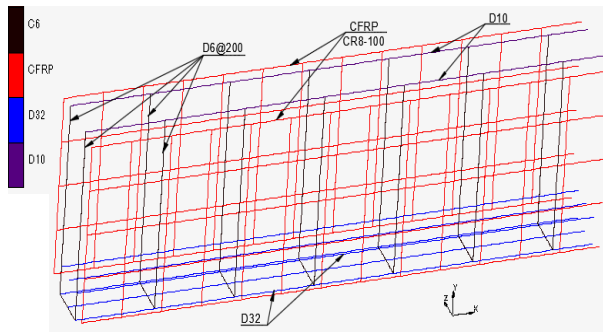


Fig. 6 Rebar and CFRP elements in models

$$E_s = \sigma_f / \varepsilon_u \quad (3)$$

Using Eq. (3), the linear tension softening behavior has been specified with a softening modulus  $E_s$  equal to 2920 N/mm<sup>2</sup> for concrete and 2870 N/mm<sup>2</sup> for mortar.

The crushing strain  $\sigma_{cu}$ , also called the ultimate compressive strain, was chosen as 0.0035 mm. This parameter is complied with the Standard Specifications for Concrete Structures [6]. Shear retention factor is 0.2, which is usually recommended for normal concrete [7]. With the polymer-modified mortar, this factor is set to zero; hence, no shear stiffness is present at an integration point once a crack occurs.

With the intention of predicting more accurately the response of concrete to loading, the Linear Mohr-Coulomb criterion was proposed to these materials. The yield stress was set to 1/3 of the compressive strength, 11.37 N/mm<sup>2</sup> and 12.23 N/mm<sup>2</sup> of the concrete and mortar material, respectively; factor  $\alpha$  (a material constant), which is obtained from tests' data, was assumed as 0.2 [8]. Other mechanical characteristics were set same as experimental values.

#### (2) Steel and CFRP

Steel and CFRP were modelled by truss elements (type 9) that embed into their corresponding solid elements (host entities: concrete and mortar), using the Links/Insert function (Fig. 6). The degrees of freedom of the nodes in the inserted node list or element list are automatically tied using the corresponding degrees of freedom of the nodes in host body elements based on their iso-parametric location in the elements. This paper focuses on evaluating the bond behavior between the repair layer (CFRP + sprayed mortar) and the substrate concrete. Therefore, for simplicity, it is assumed that there is perfect bonding between these reinforcement elements to their host entities.

Steel was defined as an elastic-plastic isotropic material with the mechanical characteristics same as in the actual experiment (Fig. 7a). Also, CFRP was defined as an elastic isotropic material (Fig. 7b).

#### (3) Bond characteristic of the interface between concrete and mortar

The bond behavior between the substrate concrete and the repair mortar were simulated by using Contact function of the program. Assuming only shear stress would work at the interface; the glued contact was

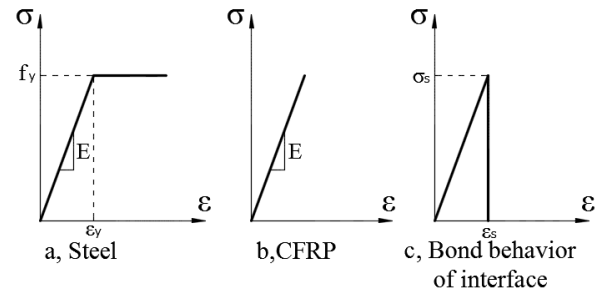


Fig. 7 Constitutive of rebar, CFRP & the interface

Table 5 Load capacity results

Type	Maximum load (kN)			%*
	Design	Test	FEM	
RC1	361	690	623	-10.8
RC2	608	757	798	5.1
RC3	523	617	731	15.5

\*%: Amount of change in analysis compared with test

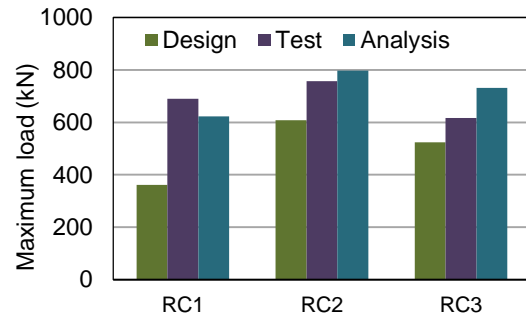


Fig. 8: Comparison of load capacity

activated between two bodies with a breaking tangential stress. When the stress of nodes at the interface reach to the critical stress  $\sigma_s$ , the glued contact will be released, it switches from glued contact to touching contact. The breaking tangential stress is 4.75 N/mm<sup>2</sup>, which obtained from the direct shear test of two materials (Fig. 7c).

### 3.2 Analysis procedure

The load steps were used for adaptive load step, which is a time/load stepping procedure that automatically changes the time step over the total time. For the convergence criterion, it was used residuals with the tolerances are 0.01; convergence will be obtained if this condition is satisfied. The full Newton-Raphson iterative technique were used to solve these models.

## 4. RESULTS AND DISCUSSIONS

Analytical predictions are compared to design and experiment's results in this section. All the tested beams and FEM models failed in shear as was expected. Specially, owing to the strong adhesion of Epoxy Primer, the bond between concrete substrate and mortar was maintained until the ultimate load in the both methods.

### 4.1 Load capacity

The detail load capacity are listed in Table 5. The shear design capacity ( $V_{yd}$ ) of beam values were calculated based on the JSCE Specification [9]. The value is basically sum of shear capacity of components

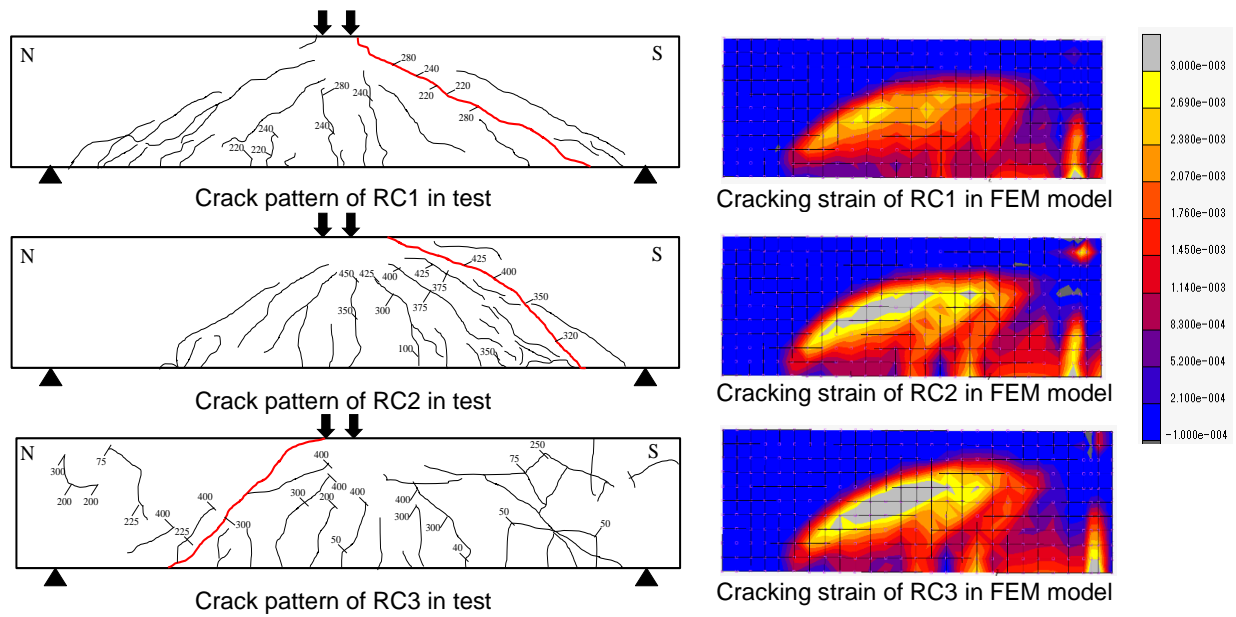


Fig. 9: Crack patterns in tests and modellings

carried by concrete ( $V_{cd}$ ), shear reinforcements ( $V_{sd}$ ) and CFRP bars ( $V_{CFRP}$ ).

Therefore, it is given as follows:

$$V_{yd} = V_{cd} + V_{sd} + V_{CFRP} \quad (4)$$

In where, CFRP bars were calculated same as steel bars.

As can be seen in Table 5 and Fig. 8, due to the safety in design standard, the design load capacity is much less than the testing and analytical results. However, in all methods, the capacity of each beam reflects relatively accurately their compositions. The normal standard beam RC1 always get the lowest result. On the other hand, beam RC2, which has both stirrups and CFRP-Mortar layer, obtained the highest load capacity. RC3, although did not use stirrup, thanks to the repair layer of CFRP and polymer mortar, it was not so weaker than the RC2 beam.

The computational analyses are shown to be good agreement with the experimental results. From Table 5, Model RC1 was failed at 623 kN, 10.8% less than the testing result. Conversely, the maximum load of model RC2 and RC3 reached to 798 kN and 731 kN; 5.1% and 15.5% higher than the experimental results, respectively.

#### 4.2 Cracks patterns and failure process

The crack patterns at failure in the tests' beam and FEM models are presented in Fig. 9. Indeed, diagonal cracks appeared in the both approaches. The propagation of cracks in different loading stages can explain the behavior of each components and the fracture mechanism. Fig. 10 shows the development of crack in the RC2 in experiment through AE events and in analysis through crack strain values. The cracks propagated similarly in the experiment and the analysis. Firstly, flexural cracks appear at the bottom-middle span of beams, and then this crack spreads horizontally at the tension area of this beam. After that, diagonal cracks are formed and develop following to the direction between

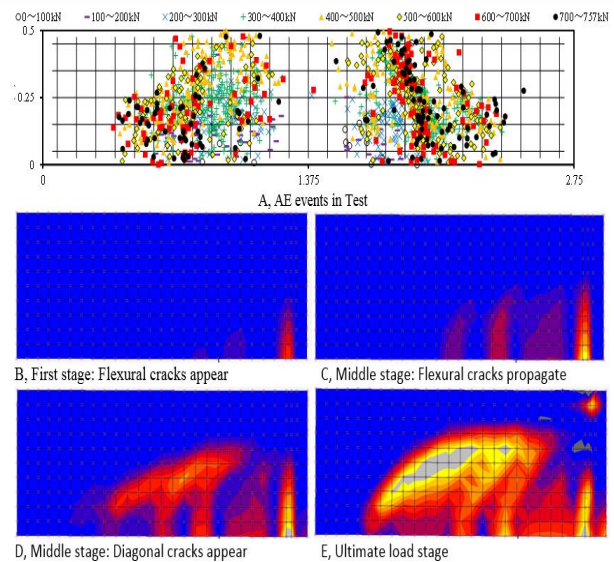


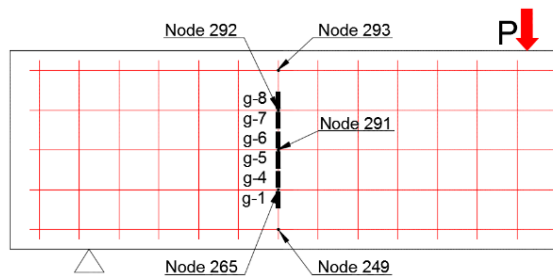
Fig. 10 Crack propagation

loading and supporting locations. Finally, this beam failed because of shear failure.

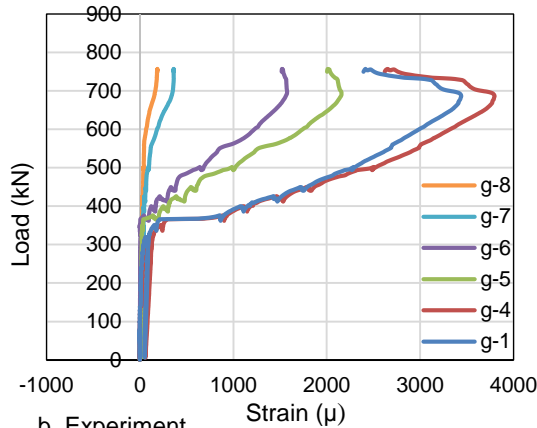
#### 4.3 Effects of CFRP grid

It is said that CFRP grid combined with sprayed mortar has been worked effectively in the repair. Obviously, using CFRP-Mortar layer provide higher load capacity not only in RC2, but also in RC3 compared to the standard beam RC1. Especially, in RC3, the initial shear crack appeared quickly (at  $\approx 75$ kN), however owing to the effect of CFRP-mortar layer, the maximum load could increase more than the value of RC1.

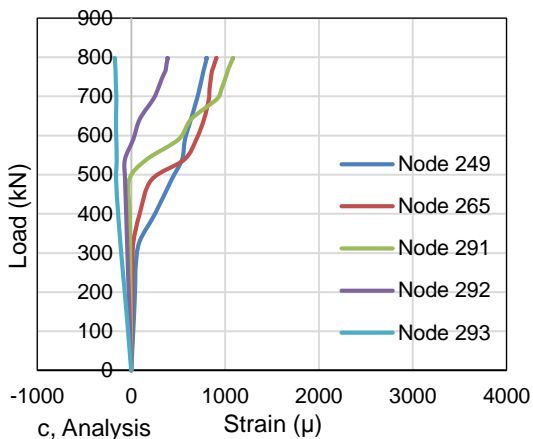
Fig. 11b,c presents strains of CFRP in RC2 monitored in the test and strains of the corresponding nodes from the modelling. Their detail location shows in Fig.11a. As can be seen, in both experimental and analytical results, strain of the CFRP bar start increasing from about over 300kN, at the moment of shear cracks appear. It proves that, CFRP grid could work together with stirrups to resist the diagonal tension stress. It is



a, Locations of sensors and model's nodes



b, Experiment



c, Analysis

Fig. 11: Behaviors of CFRP of RC2

suggested that, the CFRP grid could increase the shear stiffness of the structure. The grid would work like a system of horizontal beam and vertical truss. External stress can transmit through the grid points. Therefore, when a part of CFRP-mortar layer lose its capacity, stress will be distributed to the nearby locations. However, because of the assumption that the bond between CFRP-mortar is rigid, therefore strains of CFRP in FEM analysis are smaller than the experiment's values.

## 5. CONCLUSIONS

- (1) The load capacity of beams obtained from the four point bending test and FEM simulation are higher than the design values. This is acceptable because in design calculation, besides using many safety coefficients, shear resistance capacity only comes from concrete and shear reinforcements, not

- include tension reinforcements and others.
- (2) In this study, experimental and analytical results presented a good agreement in failure process and load capacity. These beams all failed in shear. The failure process also occurred similarity: initially, flexural cracks appeared at the middle bottom of beams; then diagonal cracks appeared at the middle of beam's web and developed to load and support locations until fail.
- (3) In addition, obviously the strengthening layer, included CFRP and sprayed mortar combined with the adhesive material Epoxy Primer, has worked efficiently in the repair work. The shear strength of these beams has significantly increased in both actual tests and simulation analysis. It is suggested that, CFRP and stirrups can work together to improve shear resistance capacity of the beams.
- (4) However, in the FEM analysis, bond behavior between each components, such as concrete-mortar, CFRP-mortar or concrete-rebar, should be studied more to simulate the actual conditions more exactly.

## ACKNOWLEDGEMENT

This research was supported by Asian Human Resources Fund from Tokyo Metropolitan Government.

## REFERENCES

- [1] Uji, K., et al. "Effects of retrofitting method using CFRP grid on shear behaviour of existing concrete members," Proceedings of the 8th International Symposium on Fiber Reinforced Polymer Reinforcement for Concrete Structures, Vol.8, 2007.
- [2] Assakkaf, I., "Shear and diagonal tension in beams," Reinforced concrete – A fundamental approach, 5<sup>th</sup> Edward G. Nawy, Prentice Hall, 2003, Chapter 6a.
- [3] Ohtsu, M., "Simplified Moment Tensor Analysis and Unified Decomposition of AE Source," Journal of Geophysical Research, Vol. 96, B4, 1991, pp. 6211-6221.
- [4] Marc-Mentat 2014, User's Manual, Vol. A, B, C, D, E, MSC Software Corporation.
- [5] Vos, E., "Influence of Loading Rate and Radial Pressure on Bond in Reinforced Concrete," PhD. Dissertation, 1983, pp.219-220.
- [6] JSCE Guidelines for Concrete, No.15: Standard Specifications for Concrete Structures, 2007, "Design", Section 5.2.3, pp 43-47.
- [7] Fehling, E., and Bullo, T., "Ultimate load capacity of reinforced steel fibre concrete deep beam subjected to shear," Finite Element in Civil Engineering Application, Hendriks & Rots, 2002.
- [8] Buyukozturk, O., "Nonlinear analysis of reinforced concrete structures," Computers & Structures, Vol. 7, 1977, pp. 149-456.
- [9] JSCE Guidelines for Concrete, No.15: Standard Specifications for Concrete Structures, 2007, "Design", Section 9.2.2.2, pp. 156-165.